An Optical Flow Based Guidance Algorithm for a Quadrotor UAV Moving Inside Circular Corridors

Amirreza Bagherzadeh[1], Fariborz Saghafi[1]

[1] Department of Aerospace Engineering, Sharif University of Technology, Tehran, Iran

Abstract

Numerous industrial corridors require inspection, traditionally conducted by human inspectors, resulting in significant time and cost, as well as potential risks of injury. To mitigate these challenges, unmanned aerial vehicles (UAVs) equipped with sensors, such as Inertial Navigation Systems (INS) and cameras, can be employed for corridor inspections. This article presents a novel guidance algorithm for quadcopter UAVs that utilizes an Optical Flow sensor. The primary objective is to autonomously guide the quadcopter UAV through the corridor, ensuring it avoids approaching the boundaries, thus minimizing the risk of collapse. To simulate the entire system, the dynamics of the UAV and the camera sensor are modeled. Furthermore, a new parameter called "relative depth" is introduced to process the optical flow, effectively reducing the impact of noise and disturbances on the optical flow data. Subsequently, the guidance algorithm, utilizing the processed "relative depth" data, is presented. Finally, extensive simulations are conducted in various corridors to test the efficacy of the algorithm, and the results are comprehensively evaluated.

Keywords: UAV; Corridors; Optical flow; Relative depth; Guidance;

1. Introduction

Currently, multirotor UAVs are extensively utilized in various industrial and hobby applications due to their rapid and autonomous capabilities in executing tasks [1]. However, their usage in indoor applications has been relatively limited. One of the main reasons for this limitation lies in their inability to utilize GPS sensors, as these sensors tend to perform poorly in indoor environments [2]. The challenges become even more pronounced in underground and industrial settings, where the absence of GPS and the compromised functionality of gyroscope sensors, especially in metallic surroundings, further exacerbate the situation. Therefore, there is a pressing need to develop new guidance systems specifically designed to operate in such challenging scenarios.

As previously mentioned, the utilization of multicopter UAVs inside confined spaces is not as widespread as outdoors. However, there is a significant interest among researchers in this field. For instance, Li, Zlatanova, Koopman, Bai, and Diakité have worked on a novel guidance algorithm for quadcopter UAVs to guide inside buildings. Their algorithm employs the A* optimization algorithm to find the optimal 3D path while avoiding collapse with obstacles [3]. In a similar vein, Krul, Pantos, Frangulea, and Valente have utilized visual data to guide quadcopters inside indoor livestock environments. They have compared the performance of two visual simultaneous localization and mapping (VSLAM), namely LSD-SLAM and ORB-SLAM, to navigate and guide the quadcopter inside a farm [4]. In addition, Padhy, Xia, Choudhury, Sa, and Bakshi have developed a new guidance algorithm that employs a camera to enable quadcopter UAVs to fly indoors. By utilizing building corners to calculate the vanishing point, the quadcopter is guided toward the vanishing point to avoid collisions with obstacles [5]. Moreover, Jano and Arogeti have developed an algorithm to navigate the quadcopter UAVs inside confined corridors. This algorithm has been adapted from the star-tracker sensor, which employs visual feature points (stars) to determine the vehicle's attitude [6].

The optical flow refers to the velocity of the image. It has been observed that various animals, including insects and birds utilize optical flow in their flight. Consequently, researchers have been interested in utilizing optical flow for guidance and navigation algorithms [7]. Serres and Ruffier have conducted a survey on the applications of optical flow in controlling and navigating UAVs and mobile robots, drawing inspiration from insects [8]. De Croon et. al have focused on integrating optical flow into their new robots resulting in a novel algorithm for calculating height by combining optical flow and control laws inspired by insects [9]. Chao, Gu, and Napolitano have worked on using the optical flow of a monocular camera mounted on a model airplane and developed a neural network to calculate optical flow and depth map from sequences of images [10]. Furthermore, Lingenfelter, Nag, and Breugel have developed an algorithm to calculate the object speed from optical flow by leveraging the vehicle's acceleration, which is sensed by an IMU subsystem. The algorithm also enables distance estimation for surrounding objects, making it suitable for obstacle avoidance [11].

From the previous research, it is evident that many of the algorithms designed to fly indoors, encounter certain common problems. Firstly, the complexity of the algorithm poses a significant issue. Algorithms relying on optimization techniques, such as A* algorithm or deep neural networks, require extensive computational power to process data and guide the vehicle. However, executing these calculations on flight computers becomes impractical due to the limited RAM capacity. Furthermore, huge calculation causes delays in control commands, which can lead to instability and failure of the vehicle, posing a risk. In the meanwhile, another challenge is accuracy. Some algorithms that rely on simplified calculations make numerous assumptions to ensure algorithm stability. Although, in the real world, these assumptions do not hold, rendering these algorithms less viable for practical use. In addition, their accuracy tends to be lower compared to other algorithms.

To address these specific challenges, our approach focuses on utilizing data obtained from optical flow to guide the UAV. Taking inspiration from insects, we process the optical flow data effectively and develop a guidance algorithm, based on this processed data. By avoiding complex computations for guidance and considering the general optical flow in data processing, we can minimize the computational cost of the algorithm. Also, this approach ensures that the accuracy of the algorithm is sufficient for guiding the UAV inside corridors. Firstly, we will present the system modeling equations and simulation process. Subsequently, we will introduce the control and guidance algorithm, which is based on optical flow. Finally, we will assess the results of the system operating inside various corridors.

2. System Modeling and Simulation

This section focuses on the modeling of the system, encompassing the dynamics of the UAV and optical flow camera. These equations serve as the foundation for simulating the system, and their outputs will be utilized in the guidance and control of the quadcopter. First, we will discuss the dynamic equations of the UAV. Following, we will present the model proposed for the camera and the image. Lastly, we will provide a procedure for generating optical flow inside a circular corridor.

2.1 The Dynamic of Quadcopter UAV

Transitional and Rotational dynamic equations for a quadrotor UAV, considering rotor inertia, are given by [12, 13]:

$$\begin{cases} \dot{u}_B = rv_B - qw_B - g\sin\theta \\ \dot{v}_B = pw_B - ru_B + g\cos\theta\sin\phi \\ \dot{w}_B = qu_B - pv_B + g\cos\theta\cos\phi + \frac{F_z}{m} \end{cases} \tag{1}$$

$$\begin{cases} \dot{p} = \left(\frac{I_{yy}-I_{zz}}{I_{xx}}\right)qr - \frac{J_p}{I_{xx}}\Omega q + \frac{M_\phi}{I_{xx}} \\ \dot{q} = \left(\frac{I_{zz}-I_{xx}}{I_{yy}}\right)pr + \frac{J_p}{I_{yy}}\Omega p + \frac{M_\theta}{I_{yy}} \\ \dot{r} = \left(\frac{I_{xx}-I_{yy}}{I_{zz}}\right)pq + \frac{M_\psi}{I_{zz}} \end{cases} \tag{2}$$

where the velocity of the body center of quadcopter wrt. the inertial frame expressed in the body coordinate system and the angular velocity of the quadcopter body frame wrt. the inertial frame expressed in the body coordinate system are given by

$$\left[\overline{v_B^I}\right]^B = [u^B \quad v^B \quad w^B],\ \left[\overline{\omega^{BI}}\right]^B = [p \quad q \quad r], \tag{3}$$

g is gravity acceleration, m is the mass of the quadcopter, F_z and $[\overline{m_{rotors}}]^B = [M_\phi \quad M_\theta \quad M_\psi]$ are thrust force and the moments produced by motors, J_p is the inertia of the rotors, Ω is equal to $\omega_4 + \omega_3 - \omega_2 - \omega_1$ and $\omega_i, i = 1 \dots 4$ are the rotor angular velocities. The thrust force and moment components of the quadcopter are determined by the angular velocity of rotors, denoted as ω_i, as well as the rotor's thrust and drag coefficient, represented by b and d.

Lastly, to model the dynamics of the actuators, the following transfer function is considered for the angular velocity of rotors:

$$\frac{\omega(s)}{\omega_c(s)} = \frac{\omega_n^2}{s^2+2\xi\omega_n s+\omega_n^2} \tag{4}$$

2.2 Camera modeling

To simulate the camera and obtain optical flow, a model for the camera is necessary. This model provides information on how the image of a point in the surroundings, such as P, will be projected onto the camera's output. The commonly used camera model is the "pinhole" model, which represents the camera as a point and a plane. This point and plane are referred to as "Camera Center" and "Camera Plane", respectively. Figure 1 depicts a schematic of the UAV, the camera center and plane, as well as the surrounding corridor.

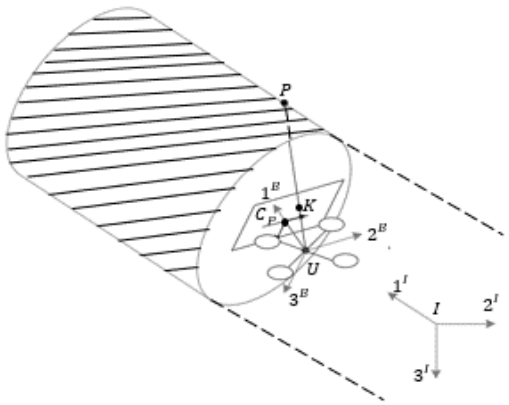

Figure 1 – Schematic of the UAV, the camera center and plane, and the surrounding corridor.

where B represents the body center of the quadcopter, assumed to be the same as the camera center, C_p denotes the center of the camera plane, P represents a point in the surrounding corridor and K corresponds to the image of the point P on the camera plane. Additionally, it is assumed that the camera's orientation aligns with the UAV's body orientation. The position of the image point K can be calculated by

$$u = f\frac{y'_{PB}}{x'_{PB}},\ v = f\frac{z'_{PB}}{x'_{PB}} \tag{5}$$

where $\left[\overline{s_{KC_p}}\right]^B = [0 \quad u \quad v]$ and $[\overline{s_{PB}}]^B = [x'_{PB} \quad y'_{PB} \quad z'_{PB}]$.

Optical flow corresponds to the velocity of the image points and can be derived from a sequence of frames. So, if the image position points in time k and $k-1$ are known, the optical flow can be calculated from

$$OF_{u,i,k} = \frac{u_{i,k} - u_{i,k-1}}{\Delta t}, \quad OF_{v,i,k} = \frac{v_{i,k} - v_{i,k-1}}{\Delta t} \tag{6}$$

where Δt is the the time between two following frames and $OF_{u,i,k}$ and $OF_{v,i,k}$ are the optical flow vector components of point i in time k in the u and v axis, respectively.

2.3 Optical Flow Simulation Inside Circular Corridor

For the sake of simplicity, this article assumes that the corridor can be divided into two types: straight corridors, which has a straight centerline, and curved corridors, where the centerline forms a sector of a circle on a specific plane. To reduce the computational cost for the simulation, the following procedure is utilized [14].

Initially, the corridor is divided into several parts. The rationale behind this division will be discussed subsequently. Next, the distance between the UAV and the centerline of each part is calculated. The UAV is considered to be in the part with the minimum distance. Also, if the minimum distance between the UAV and the centerlines of the sections is greater than or equal to the radius of the corridor, a collision is detected and the simulation is halted. For each part in which the UAV is located and the subsequent parts, the following steps are performed:

1. For any image point on the camera plane, if the corresponding point is not defined, do the steps (2) and (3). Nevertheless, continue the loop.
2. Calculate $\left[s_{K_iB}\right]^B$ for every image point mentioned in step (a).
3. Draw a line from B to K_i and extend it until intersects with the specified part. If the line hits the part, denote the intersection point as P_i and calculate $\left[s_{P_iI}\right]^I$.

Subsequently, move to the next time step (after Δt seconds) and obtain a new position and orientation of the UAV. Denote the new UAV's body center as B' and the new body coordinate system as B'. For any image point that has a corresponding surrounding point, calculate $\left[s'_{K_i'B'}\right]^{B'}$ as

$$\left[s'_{K_i'B'}\right]^{B'} = \begin{bmatrix} f \\ u_i' \\ v_i' \end{bmatrix} = \frac{f}{x_i'} \begin{bmatrix} x_i' \\ y_i' \\ z_i' \end{bmatrix}; \quad \left[s_{P_iB'}\right]^{B'} = \begin{bmatrix} x_i' \\ y_i' \\ z_i' \end{bmatrix} \tag{7}$$

Finally, determine optical flow as:

$$OF_{u_i} = \frac{u_i' - u_i}{\Delta t}, \quad OF_{v_i} = \frac{v_i' - v_i}{\Delta t} \tag{8}$$

3. Quadcopter Guidance and control

This section focused on the guidance and control of the quadcopter UAV. Firstly, the calculation of optical flow in a general form will be discussed, followed by the extraction of its components. Consequently, the concept of "relative depth" will be defined, and the procedure for calculating the relative depth will be derived. Next, the control strategy, to generate reliable optical flow for utilizing inside the guidance subsystem, will be explored. Finally, the guidance law inside a circular corridor using relative depth will be specified.

3.1 Optical flow in general form

By calculating the derivatives of the image location (u, v) and assuming that the position of the corridor's points remains constant over time, it can be shown that

$$OF_{u,i,k} = \frac{u_{i,k} - u_{i,k-1}}{\Delta t}, \quad OF_{v,i,k} = \frac{v_{i,k} - v_{i,k-1}}{\Delta t} \tag{9}$$

Hence, $(u_0, v_0) = (fv_B/u_B, fw_B/u_B)$ represents the "Focus of Expansion (FOE)". It is worth noting that optical flow consists of two components: rotational optical flow and transitional optical flow. The rotational optical flow is generated by the angular velocity of the camera, while the transitional optical flow is formed due to the location of the surrounding point relative to the body center of the camera.

Research has shown that insects primarily rely on transitional optical flow during flight, and their ability to previse visual information declines significantly when they experience angular velocity [14]. This observation offers a valuable technique for utilizing optical flow in UAV guidance. Similar to insects, if the impact of angular velocity on optical flow falls below a certain threshold, the optical flow is considered reliable and can be incorporated inside the guidance law, resulting in a change in the guidance output. Conversely, if the angular velocity's effect on the optical flow exceeds the threshold, the optical flow becomes unreliable, rendering the guidance law ineffective, and the guidance output remains constant. To determine the extent of the angular effect on optical flow, a specific parameter will be established later.

3.2 Relative Depth

As discussed previously, the primary objective of processing optical flow is to determine a quantity that solely reflects the environment and is independent of the quadcopter's dynamic states or the location of the image point. Assuming the angular velocity of the quadcopter is zero, we can evaluate the following expressions from (9):

$$OF_u = \frac{u_B(u-u_0)}{x'_{PB}}, \quad OF_v = \frac{u_B(v-v_0)}{x'_{PB}} \tag{10}$$

Introducing the relative depth as $RD \triangleq 1/x'_{PB}$, we can determine the relative depth using

$$RD = \frac{[OF_u(u-u_0)+OF_v(v-v_0)]}{u_B[(u-u_0)^2+(v-v_0)^2]} \tag{11}$$

To evaluate the pair (u_0, v_0) for calculating the relative depth, equation (10) shows that the best estimation (u_0^*, v_0^*) can be calculated using the following equation [15]:

$$\begin{bmatrix} u_0^* \\ v_0^* \end{bmatrix} = \begin{bmatrix} OF_{v_1} & -OF_{u_1} \\ \vdots & \vdots \\ OF_{v_N} & -OF_{u_N} \end{bmatrix}^{\dagger} \begin{bmatrix} OF_{v_1}u_1 - OF_{u_1}v_1 \\ \vdots \\ OF_{v_N}u_N - OF_{u_N}v_N \end{bmatrix} \tag{12}$$

Hence, N shows the total count of the image points and for matrix A, $A^{\dagger}$ denotes the pseudo inverse of the matrix A which has been defined as:

$$A^{\dagger} = (A^T A)^{-1} A^T \tag{13}$$

As mentioned earlier, it is necessary to determine the impact of angular velocity on the optical flow. To quantify this effect, we introduce a new term called the "Rotational Error of Optical Flow" as

$$Err = \frac{1}{N}\sum_i \left| OF_{u_i}(v_i - v_0) - OF_{v_i}(u_i - u_0) \right|. \tag{14}$$

This quantity is non-negative, as it involves the use of the absolute function. Furthermore, it approaches zero when the angular velocity is zero (by substituting (10) into (13)). Therefore, if the value of this term falls below a specified threshold, we can assume that the effect of angular velocity is negligible.

3.3 Control strategy for quadcopter UAV

This section discusses the control strategy for the quadcopter. It is important to note that, unlike guidance methods with static images, the quadcopter needs to gain speed to generate reliable optical flow for guidance. In other words, the guidance system does not function effectively when the quadcopter remains stationary. So, the optimal trajectory for the quadcopter to produce a stable optical flow is a straight line, maintaining a constant speed without orientation changes. This speed is necessary to produce effective optical flow. In our mission, the best-desired path is the centerline of the circular corridor, which offers the maximum distance from the surrounding obstacles. To ensure a constant speed, the desired pitch and roll angles for the quadcopter are set to $\theta_{des} = \phi_{des} = 0$.

To simplify the control, we employ the two-cascaded PID control loop to stabilize and control the quadcopter's trajectory. Rather than directly controlling three desired coordinate positions and heading angle in the outer loop, it is more practical and straightforward to control the speed component along the first axis of the body coordinate system (u_{des}), the desired heading angle (ψ_{des}), and the variables y' and z', defined as:

$$y'(t) = \int_0^t v_B \, dt, \quad z'(t) = \int_0^t w_B \, dt. \tag{15}$$

In the circular corridor, the guidance system provides information about the deviation of the quadcopter's heading from the corridor's orientation (indicated by two angles ψ_{obs} and θ_{obs}) and the displacement of the quadcopter from the corridor's centerline (represented by two distances y'_{obs} and z'_{obs}). When these observed variables are zero, it indicates that the quadcopter is precisely on the centerline of the corridor and moving through it. Therefore, the control law for y' and z' can be defined as follows:

$$y'_{des} = y' - y'_{obs}, \quad z'_{des} = z' - z'_{obs} \tag{16}$$

Through this control law, it can be affirmed that in any situation, the position error in this system will decrease, eventually reaching zero. To track the centerline of corridors that inclines or declines (in the z-axis), resulting in non-zero θ_{obs}, the control low for z'_{des} will be modified as follows:

$$\dot{z'}_{des} = V \tan\theta_{obs} \quad \& \quad z'_{des,new} = \frac{z'_{des}}{\cos\theta_{obs}} \tag{17}$$

3.4 Guidance law for quadcopter UAV

In this section, we will discuss the guidance law of the quadcopter UAV. The guidance law plays a crucial role in determining the heading and pitch angle of the attitude of quadcopter wrt. the centerline of the corridor. Additionally, it calculates components of the displacement of the quadcopter's body center from the corridor centerline in the body coordinate system. Furthermore, we will explore a guidance law in order to apply the guidance output values to the control loop so the stability and convergence of the system will be guaranteed.

The minimum relative depth signifies the point farthest from the quadcopter, which needs to be reached to avoid the surroundings (like the vanishing point in [5]). When the image of this point is centered inside the camera plane, this objective is achieved. Simulating optical flow inside a circular corridor reveals that only deviation in the heading and pitch angle affect the location of the minimum relative depth point, while displacement does not alter its position. Therefore, the initial step involves identifying a suitable candidate for this point, that is less susceptible to errors and noise. To accomplish this, consider the points that satisfy the following equation:

$$RD(i,j) < p * (RD_{max} - RD_{min}) + RD_{min} \tag{18}$$

Hence, $p \in [0,1]$ is a small parameter, (RD_{max}, RD_{min}) is maximum and minimum relative depth value in the map. Then, calculate the mean position ($\bar{u}$ and $\bar{v}$) of these points from the center point. The angles can be determined using the following expression:

$$\psi_{obs} = \tan^{-1}\frac{\bar{u}}{f}, \quad \theta_{obs} = \tan^{-1}\frac{\bar{v}}{\sqrt{f^2+\bar{u}^2}} \tag{19}$$

To determine the quadcopter's displacement, the surrounding points in the image with the shortest distance from the camera and consequently the greatest optical flow and relative depth are utilized. Assuming zero heading and pitch angle deviation and employing (10), these points lie on the circular section of the corridor. It can be verified that:

$$\begin{bmatrix} 2y'_{P_1B} & 2z'_{P_1B} & 1 \\ \vdots & \vdots & \vdots \\ 2y'_{P_NB} & 2z'_{P_NB} & 1 \end{bmatrix} \begin{bmatrix} y'_{C'B} \\ z'_{C'B} \\ R^2 - y'^2_{C'B} - z'^2_{C'B} \end{bmatrix} = \begin{bmatrix} y'^2_{P_1B} + z'^2_{P_1B} \\ \vdots \\ y'^2_{P_NB} + z'^2_{P_NB} \end{bmatrix} \tag{20}$$

Hence, using (19) and calculating y'_{P_iB} and z'_{P_iB} from RD_i, u_i, and v_i, the best estimation for the quadcopter's displacement ($y'_{C'B}$ and $z'_{C'B}$) can be determined by:

$$\begin{bmatrix} {y'}^{*}_{C'B} \\ {z'}^{*}_{C'B} \\ R^{*2} - {y'}^{*2}_{C'B} - {z'}^{*2}_{C'B} \end{bmatrix} = \begin{bmatrix} 2y'_{P_1B} & 2z'_{P_1B} & 1 \\ \vdots & \vdots & \vdots \\ 2y'_{P_NB} & 2z'_{P_NB} & 1 \end{bmatrix}^{\dagger} \begin{bmatrix} {y'}^{2}_{P_1B} + {z'}^{2}_{P_1B} \\ \vdots \\ {y'}^{2}_{P_NB} + {z'}^{2}_{P_NB} \end{bmatrix} \tag{21}$$

It's important to note that the equations mentioned above are applicable when the optical flow remains reliable, with a rotational error of the optical flow below a specified threshold. Therefore, it is crucial to determine the desired values to be applied to the control loop only when the optical flow remains reliable for a certain period of time. Furthermore, to prevent the system from diverging and ensure stability around the centerline, upper and lower saturation values are utilized for the desired values. As a result, the following guidance law is employed for the guidance output values:

- Given the specified frequency f_g, the error value of the optical flow is checked.
- If the error (Err) remains below a threshold value thr_{Err} for all N steps, the following actions are performed:
    - Calculate the average of the angle values, denoted as $\bar{\psi}_{obs}$ and $\bar{\theta}_{obs}$.
    - Take the last value of the distance values, denoted as y'_{obs} and z'_{obs}.
    - Modify the desired values of angles and distances (for the control loop) using the following equations:

$$\psi_{des} \leftarrow \psi_{des} - \psi_{obs,1}; \quad \psi_{obs,1} = \begin{cases} 0; & |\bar{\psi}_{obs}| \le \psi_1 \\ \bar{\psi}_{obs}; & \psi_1 < |\bar{\psi}_{obs}| \le \psi_2 \\ \psi_2; & \bar{\psi}_{obs} > \psi_2 \\ -\psi_2; & \bar{\psi}_{obs} < -\psi_2 \end{cases} \tag{22}$$

$$\theta_{des} \leftarrow \theta_{obs,1}; \quad \theta_{obs,1} = \begin{cases} 0; & |\bar{\theta}_{obs}| \le \theta_1 \\ \bar{\theta}_{obs}; & \theta_1 < |\bar{\theta}_{obs}| \le \theta_2 \\ \theta_2; & \bar{\theta}_{obs} > \theta_2 \\ -\theta_2; & \bar{\theta}_{obs} < -\theta_2 \end{cases} \tag{23}$$

$$y'_{des} \leftarrow y'_{des} - y'_{obs,1}; \quad y'_{obs,1} = \begin{cases} 0; & |y'_{obs}| \le y'_1 \\ y'_{obs}; & y'_1 < |y'_{obs}| \le y'_2 \\ y'_2; & y'_{obs} > y'_2 \\ -y'_2; & y'_{obs} < -y'_2 \end{cases} \tag{24}$$

$$z'_{des} \leftarrow z'_{des} - z'_{obs,1}; \quad z'_{obs,1} = \begin{cases} 0; & |z'_{obs}| \le z'_1 \\ z'_{obs}; & z'_1 < |z'_{obs}| \le z'_2 \\ z'_2; & z'_{obs} > z'_2 \\ -z'_2; & z'_{obs} < -z'_2 \end{cases} \tag{25}$$

4. Simulation and Results

In this section, we evaluate the results from simulating the quadcopter UAV inside a circular corridor. Initially, we provide the parameters of the UAV and the camera. Subsequently, we analyze the optical flow and relative depth inside the straight corridor using a predefined trajectory. Finally, we assess the performance of the guidance system across different types of corridors.

4.1 UAV and Camera Parameters

The parameters for the UAV dynamics and the camera modeling are provided in Table 1.

Table 1 – UAV and camera modeling parameters

Parameter	Value	Parameter	Value
m	$2\ kg$	b	$9.6 \times 10^{-6}\ N \cdot s^2$
I_{xx}	$0.0035\ kg \cdot m^2$	l	$0.225\ m$
I_{yy}	$0.0035\ kg \cdot m^2$	ω_{max}	$9600\ RPM$
I_{zz}	$0.005\ kg \cdot m^2$	$\omega_{n,rotor}$	141.44
J_p	$2.8 \times 10^{-6}\ kg \cdot m^2$	ξ_{rotor}	0.707
d_f	$1.57 \times 10^{-7}\ N \cdot m \cdot s^2$	f_1	$3.6\ mm$
f_g	$5\ Hz$	thr_{Err}	0.3
N	5	ψ_1	4°
ψ_2	30°	θ_1	10°
y_1'	$2\ cm$	θ_2	20°
y_2'	$50\ cm$	z_1'	$2\ cm$
z_2'	$50\ cm$		
Camera's window size	52×36	Length of any pixel	$70\ \mu m$

4.2 Optical flow and relative depth in a circular corridor

To understand the optical flow behavior inside the circular corridor, we create a pre-defined trajectory for the quadcopter and simulate it inside a straight corridor. This allowed us to observe the optical flow's response. The trajectory has been defined by:

$$x = \begin{cases} 0; & t \le 10 \\ t - 10; & t \ge 10 \end{cases}, \quad y = \begin{cases} 0; & t < 20 \\ 0.5; & 20 \le t \le 40 \\ 0; & t > 40 \end{cases}, z = \begin{cases} 1.5; & t < 20 \\ 2; & 20 \le t \le 40 \\ 1.5; & t > 40 \end{cases} \tag{26}$$

To observe the results and the mentioned effect, we have provided videos showcasing the optical flow and relative depth (here and here). Upon reviewing these videos, it becomes apparent that when the UAV flies in a straight line at a constant speed, the optical flow is totally transitional and the relative depth accurately represents the distance of the surrounding points. However, when the UAV changes its position (at $t = 20$ and $t = 40$), the rotational component of optical flow becomes noticeable, resulting in sudden changes in the relative depth. After a short period, the rotational component diminishes, and the relative depth performance returns to normal. This observation is also evident from the plot depicting the "Rotational error of optical flow" over time (Figure 2).

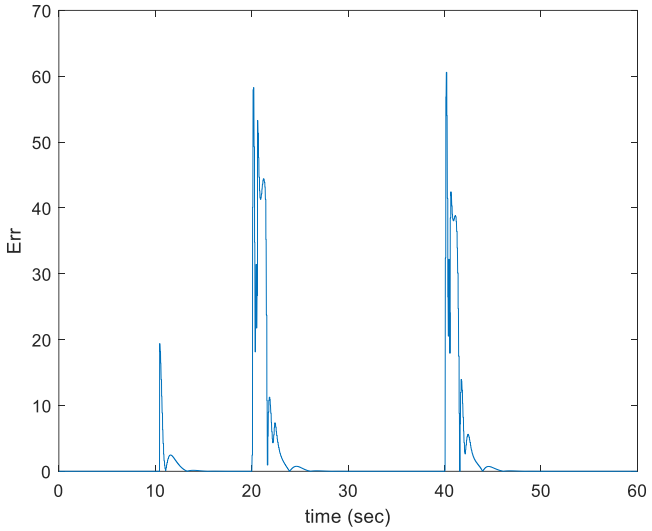

Figure 2 – Plot of rotational error of optical flow versus time.

The term mentioned above can serve as an indicator of the optical flow's transitional or rotational nature. As explained earlier, when this term falls below a certain threshold, the information obtained from the relative depth becomes suitable for guiding the UAV system.

4.3 Simulation of UAV system inside various corridors

This section presents the results of the UAV simulation conducted in various corridors. To assess the guidance algorithm's ability to avoid collisions with the corridor surroundings, the following procedure was followed for each simulation.

Initially, the quadcopter is positioned one meter below the centerline on the stand. The first part of the corridor is assumed to be straight for a distance of 30 meters. At the start of the simulation, the quadcopter elevates and hovers along the centerline of the corridor. At $t = 10\ sec$, the quadcopter proceeds through the corridor at a speed of $25\ cm/sec$. At $t = 20\ sec$, the quadcopter experiences a half-meter displacement in the positive y and z axis. At $t = 30\ sec$, the quadcopter adjusts its heading angle to $10°$. At $t = 40\ sec$, the quadcopter's guidance system becomes active.

To challenge the guidance system in different scenarios, four distinct corridors were considered: A straightforward corridor with a length of 300 meters, named as straight corridor, a straight corridor with a length of 30 meters, followed by a straight corridor that bends up to 60 degrees, named as bent corridor, a straight corridor with a length of 30 meters, connected to a curved corridor with a radius of 10 meters, and finally connected to another long straight corridor, named as bent corridor, and lastly, a straight corridor with a length of 30 meters, followed by a 20-meter straight corridor with a 30-degrees ramp ($+z$ angle), and another straight corridor parallel to the first one, named as ramped corridor.

All simulations were conducted with corridors which the radius of the corridor's section is 2 meters. The duration of the straight corridor simulation was 120 seconds, while the others lasted for 250 seconds. Figures 3, 4, 5 and 6 provide the results of these simulations. The results demonstrate the effectiveness of the optical flow-based guidance algorithm for a quadcopter flying inside a circular corridor. This algorithm can accurately detect the displacement and attitude errors relative to the corridor and, over time, successfully track the centerline of the circular corridor.

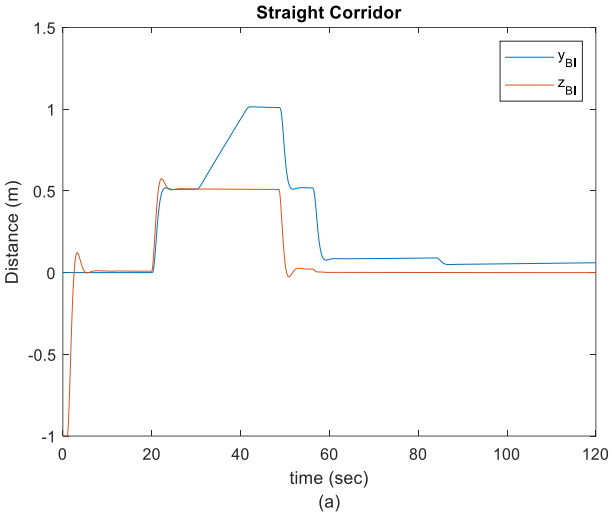

Figure 3 – Plot of y_{BI} and z_{BI} of UAV versus time inside straight corridor

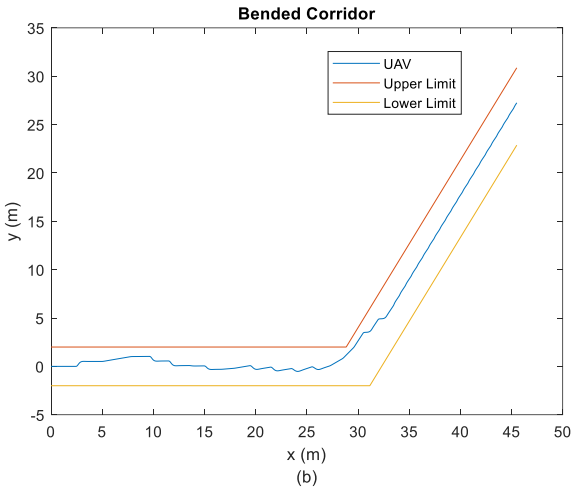

Figure 4 – Plot of y_{BI} of UAV versus x_{BI} inside bent corridor.

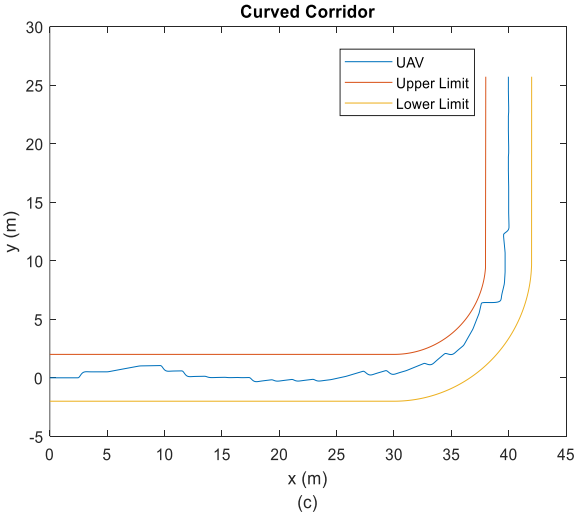

Figure 5 – Plot of y_{BI} of UAV versus x_{BI} inside curved corridor.

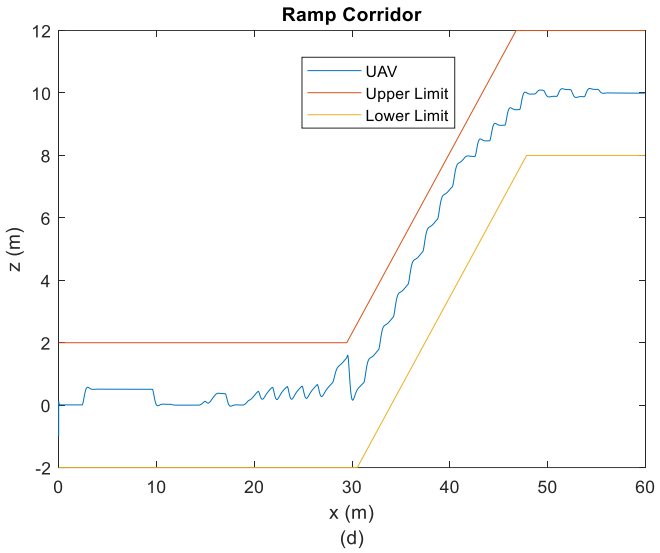

Figure 6 – Plot of z_{BI} of UAV versus x_{BI} inside ramp corridor

5. Conclusions

This article presents the development of a novel guidance algorithm based on optical flow. Inspired by insects, we introduce a new quantity called "relative depth" to capture transitional optical flow. This computationally efficient quantity provides information about the distance of each surrounding point in the image, enabling safe navigation of a robot within a 3D environment, while avoiding collisions.

Furthermore, the concept of "rotational error on optical flow" as a means to assess the impact of angular velocity on optical flow is introduced. This measure allows us to determine the reliability of the relative depth and its suitability for integration into the guidance algorithm. By considering a circular corridor as the environment, our proposed guidance algorithm utilizes these terms to guide the quadcopter safely, preventing collisions.

To evaluate the effectiveness of this guidance algorithm, many tests were conducted in various types of corridors. The results demonstrate that the algorithm effectively corrects both attitude and position errors simultaneously, enabling the system to fly with a constant speed along the centerline of the corridor, thereby ensuring the safety of the UAV system.

6. Contact Author Email Address

mailto: amirreza.bagherzadeh@ae.sharif.edu or saghafi@sharif.edu

7. Copyright Statement

References

[1] Tiago P. Nascimento and M. Saska. Position and attitude control of multi-rotor aerial vehicles: A survey. *Annual Reviews in Control*, Vol. 48, pp. 129-14, August 2019.

[2] H. Bavle, J. L. Sanchez-Lopez, A. Rodriguez-Ramos, C. Sampedro and P. Campoy. A flight altitude estimator for multirotor UAVs in dynamic and unstructured indoor environments. *2017 International Conference on Unmanned Aircraft Systems (ICUAS)*, Miami, FL, USA, pp. 1044-1051, June 2017.

[3] F. Li, S. Zlatanova, M. Koopman, X. Bai and A. Diakité. Universal path planning for an indoor drone. *Automation in Construction*, Vol. 95, pp.275-283, 2018.

[4] S. Krul, C. Pantos, M. Frangulea and J. Valente. Visual SLAM for indoor livestock and farming using a small drone with a monocular camera: A feasibility study. *Drones*, Vol. 5, no. 2, p. 41, 2021.

[5] R.P. Padhy, F. Xia, S.K. Choudhury, P.K. Sa and S. Bakshi. Monocular vision aided autonomous UAV navigation in indoor corridor environments. *IEEE Transactions on Sustainable Computing*, Vol. 4, no. 1, pp. 96-108, 2018.

[6] D. Jano, and S. Arogeti. Drone's Attitude Estimation in Corridor-Like Environments. *2019 European Conference on Mobile Robots (ECMR)*, pp. 1-6. IEEE, 2019.

[7] F. Kendoul, I. Fantoni and K. Nonami. Optic flow-based vision system for autonomous 3D localization and control of small aerial vehicles. *Robotics and autonomous systems*, Vol. 57, no. 6-7, pp. 591-602, 2009.

[8] J.R. Serres and F. Ruffier. Optic flow-based collision-free strategies: From insects to robots. *Arthropod structure & development*, Vol. 46, no. 5, pp.703-717, 2017.

[9] G. C.H.E. De Croon, J. JG Dupeyroux, C. De Wagter, A. Chatterjee, D. A. Olejnik, and F. Ruffier. Accommodating unobservability to control flight attitude with optic flow. *Nature*, Vol. 610, No. 7932, pp. 485-490, 2022.

[10] H. Chao, Y. Gu and M. Napolitano. A survey of optical flow techniques for UAV navigation applications. *2013 International Conference on Unmanned Aircraft Systems (ICUAS)*, IEEE, pp. 710-716, May 2013.

[11] B. Lingenfelter, A. Nag and F. van Breugel. Insect inspired vision-based velocity estimation through spatial pooling of optic flow during linear motion. *Bioinspiration & Biomimetics*, Vol. 16, No. 6, page 066004, 2021.

[12] P. H. Zipfel. *Modeling and Simulation of Aerospace Vehicle Dynamics*. Second Edition, AIAA, 2007.

[13] D. Bhattacharjee and K. Subbarao. Robust control strategy for quadcopters using sliding mode control and model predictive control. *AIAA Scitech 2020 Forum*, page 2071, 2020.

[14] M. Rezaei. *Optical flow based flight of a small fixed-wing aircraft in ideal urban environments*. Master Thesis, Sharif University of Technology, June 2011.

[15] P. Agrawal, A. Ratnoo and D. Ghose. Inverse optical flow based guidance for UAV navigation through urban canyons. *Aerospace Science and Technology*, Vol. 68, pp. 163-178, 2017.